Earth and Planetary Science Letters 390 (2014) 69–79

Contents lists available at ScienceDirect

Earth and Planetary Science Letters

www.elsevier.com/locate/epsl

Changes in ITCZ location and cross-equatorial heat transport at the Last Glacial Maximum, Heinrich Stadial 1, and the mid-Holocene

David McGee *, Aaron Donohoe, John Marshall, David Ferreira [1]

Department of Earth, Atmospheric and Planetary Sciences, Massachusetts Institute of Technology, Cambridge, MA 02139, USA

ARTICLE INFO

Article history:
Received 10 August 2013
Received in revised form 20 December 2013
Accepted 27 December 2013
Available online 21 January 2014
Editor: J. Lynch-Stieglitz

Keywords:
ITCZ
heat transport
Heinrich events
Last Glacial Maximum
mid-Holocene

ABSTRACT

Tropical paleoclimate records provide important insights into the response of precipitation patterns and the Hadley circulation to past climate changes. Paleo-records are commonly interpreted as indicating north–south shifts of the Intertropical Convergence Zone (ITCZ), with the ITCZ's mean position moving toward the warmer hemisphere in response to changes in cross-equatorial temperature gradients. Though a number of records in tropical Central and South America, North Africa, Asia and the Indo-Australian region are consistent with this interpretation, the magnitudes and regional variability of past ITCZ shifts are poorly constrained. Combining estimates of past tropical sea surface temperature (SST) gradients with the strong linear relationship observed between zonally averaged ITCZ position and tropical SST gradients in the modern seasonal cycle and in models of past climates, we quantify past shifts in zonally averaged ITCZ position. We find that mean ITCZ shifts are likely less than 1° latitude during the Last Glacial Maximum (LGM), Heinrich Stadial 1 (HS1) and mid-Holocene (6 ka) climates, with the largest shift during HS1. The ITCZ's position is closely tied to heat transport between the hemispheres by the atmosphere and ocean; accordingly, these small mean ITCZ shifts are associated with relatively large (~0.1–0.4 PW) changes in cross-equatorial atmospheric heat transport (AHT_{EQ}). These AHT_{EQ} changes point to changes in cross-equatorial ocean heat transport or net radiative fluxes of the opposite sign. During HS1, the increase in northward AHT_{EQ} is large enough to compensate for a partial or total shutdown in northward heat transport by the Atlantic Ocean's meridional overturning circulation. The large AHT_{EQ} response for small changes in mean ITCZ position places limits on the magnitude of past shifts in the globally averaged ITCZ. Large ($\geqslant 5°$) meridional displacements of the ITCZ inferred from regional compilations of proxy records must be limited in their zonal extent, and ITCZ shifts at other longitudes must be near zero, for the global mean shift to remain $\leqslant 1°$ as suggested by our results. Our examination of model results and modern observations supports variable regional and seasonal changes in ITCZ precipitation. This work thus highlights the importance of a dense network of tropical precipitation reconstructions to document the regional and seasonal heterogeneity of ITCZ responses to past climate changes.

1. Introduction

Proxy records of past precipitation changes in the tropics show pronounced sensitivity to changes in cross-equatorial temperature gradients, with precipitation decreasing in the tropics of the cooler hemisphere (Fig. 1) (e.g., Clark et al., 2012; Escobar et al., 2012; Partin et al., 2007; Peterson et al., 2000; Wang et al., 2004; Weldeab et al., 2007). These records are commonly interpreted as representing changes in the local summer position of the band of heavy precipitation associated with the Intertropical Convergence Zone (ITCZ). During Heinrich Stadial 1 (HS1; ~15–18 ka), a period of cold North Atlantic sea surface temperatures (SSTs) and rising temperatures in the Southern Hemisphere (Bard et al., 2000; Monnin et al., 2001; Shakun et al., 2012), sites in the northern tropics show evidence for reduced precipitation, weakened summer monsoons and increased winter trade winds (Escobar et al., 2012; Gibbons et al., 2014; McGee et al., 2013; Peterson et al., 2000; Rashid et al., 2011; Wang et al., 2001; Weldeab et al., 2007), and several sites in central South America and northern Australia suggest increased precipitation (Ayliffe et al., 2013; Cruz et al., 2005; Denniston et al., 2013; Kanner et al., 2012; Muller et al., 2008; Placzek et al., 2006; Wang et al., 2004). Both of these sets of observations are consistent with a southward displacement of the ITCZ's seasonal range in conjunction with a negative (cooler North, warmer South) cross-equatorial temperature gradient.

An opposite pattern is observed during the mid-Holocene (6–8 ka), a time when northern hemisphere (NH) summer occurred near perihelion. Sites in the northern tropics record higher

* Corresponding author.
E-mail address: davidmcg@mit.edu (D. McGee).
[1] Present address: Department of Meteorology, University of Reading, UK.

0012-821X/$ – see front matter
http://dx.doi.org/10.1016/j.epsl.2013.12.043

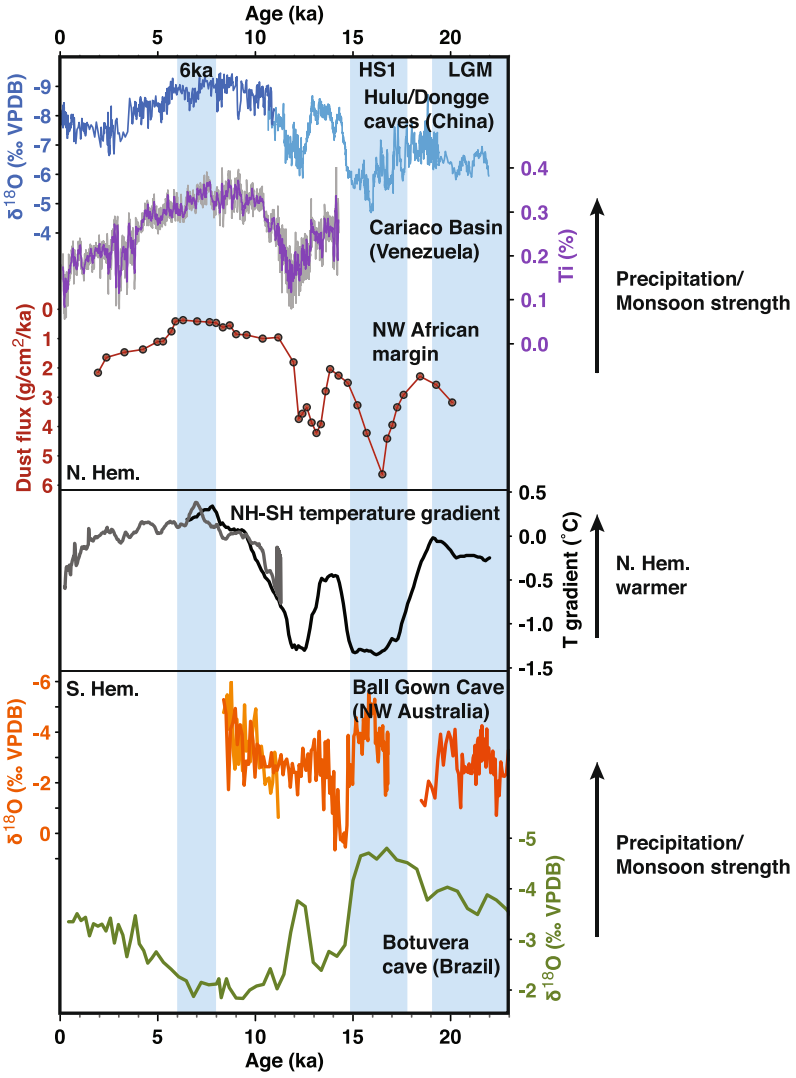

Fig. 1. Variations in inferred tropical precipitation and cross-equatorial temperature gradients over the last 25 ka. The records suggest antiphasing of tropical precipitation intensity between the hemispheres during periods of strong temperature gradients, in particular Heinrich Stadial 1 (HS1), and the mid-Holocene (6 ka), consistent with movements of the mean annual position of the ITCZ toward the warmer hemisphere. (Top) Three representative proxy records from the Northern Hemisphere tropics: speleothem $\delta^{18}O$ from Hulu and Dongge Caves, a measure of East Asian monsoon strength (Dykoski et al., 2005; Wang et al., 2001); titanium concentration in Cariaco Basin sediments, reflecting river discharge from northern South America (Haug et al., 2001); Saharan dust deposition along the NW African margin (reversed axis), reflecting summer precipitation and winter trade wind intensity (McGee et al., 2013). (Center) Reconstructions of whole-hemisphere surface temperature gradients expressed as the area-weighted mean NH surface temperature minus SH surface temperature, each expressed relative to the mean gradient between 11 and 6.5 ka (black: Shakun et al., 2012; grey: Marcott et al., 2013). (Bottom) Two records from the Southern Hemisphere tropics: $\delta^{18}O$ records from multiple speleothems from Ball Gown Cave in northwestern Australia (Denniston et al., 2013); and speleothem $\delta^{18}O$ from Botuvera cave in SE Brazil, reflecting summer monsoon intensity in the southern tropics of South America (Wang et al., 2007).

precipitation and reduced winter trade winds (Adkins et al., 2006; Dykoski et al., 2005; Fleitmann et al., 2007; Gasse, 2000; Haug et al., 2001; Weldeab et al., 2007), while South American sites south of the equator suggest reduced precipitation and a weaker summer monsoon (Fig. 1) (Cruz et al., 2005; Seltzer et al., 2000).

The spatial coherence of these changes seems to point to large-scale changes in ITCZ position. Accordingly, tropical precipitation paleo-records are commonly interpreted as reflecting meridional "shifts" in the ITCZ. As the ITCZ's seasonal migration determines the seasonality, intensity and spatial distribution of precipitation throughout the tropics, there is widespread interest in understanding the magnitude and character of these shifts and in determining their sensitivity to external forcings. However, presently available records are unable to constrain the magnitude of past changes in the ITCZ's seasonal range or annual-mean position. Taking HS1 as an example, we have little indication of whether drying in northern tropical sites at HS1 reflects a southward shift of the ITCZ's boreal summer position by several degrees of latitude or only a modest reduction in the amount of time spent by the ITCZ at its boreal summer extreme. Further complicating interpretation of paleo-records is the fact that changes in tropical precipitation patterns are likely to be zonally heterogeneous. During HS1, proxy data suggest something like a shift of the ITCZ at some longitudes, while in other regions precipitation decreased both north and south of the equator (Stager et al., 2011). Similarly, in recent interannual variability, 1° shifts of the mean ITCZ are associated with up to 5° shifts in some regions and little change in others (Fig. 2). Constraints on the mean ITCZ position in past climates would help us determine whether large regional ITCZ shifts reconstructed from proxy records (e.g., Arbuszewski et al., 2013; Sachs et al., 2009) represent global-scale changes or regional variability.

The position of the ITCZ is also closely tied to hemispheric energy budgets through its role in cross-equatorial atmospheric heat transport (AHT_{EQ}). In the solsticial seasons, the Hadley circulation

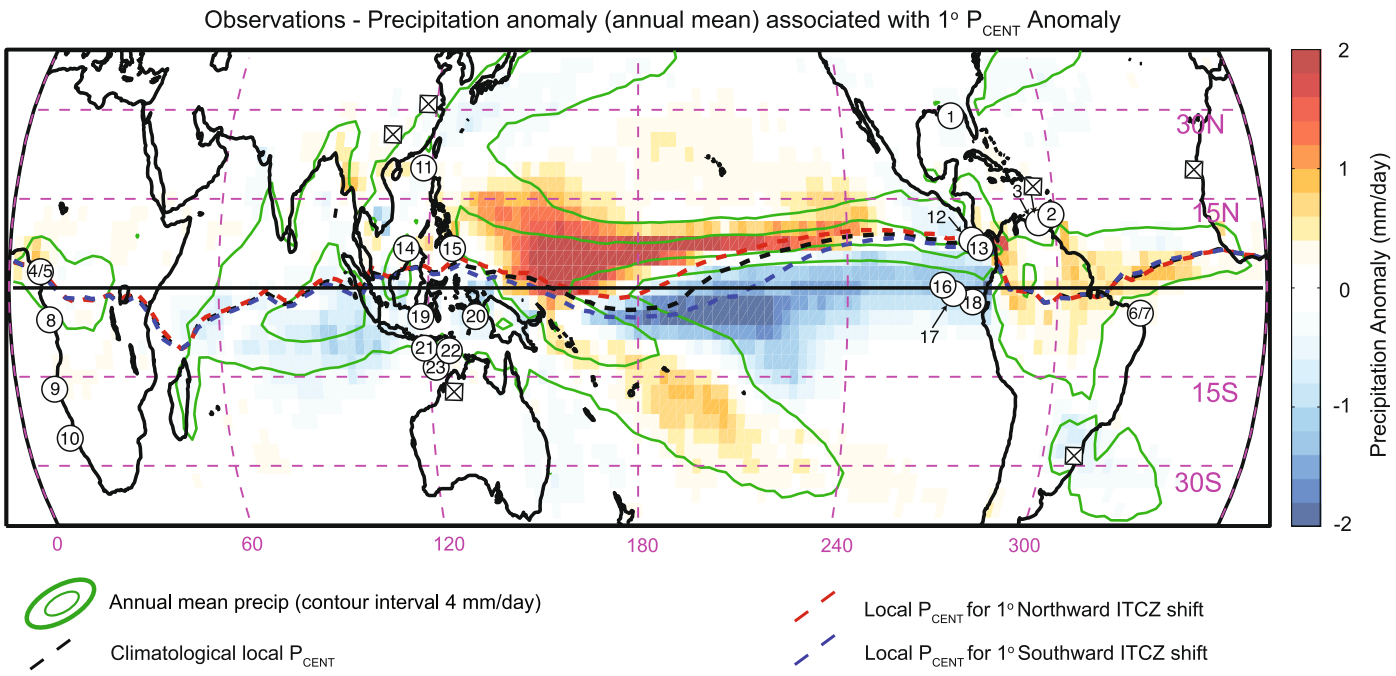

Fig. 2. Proxy data sites and regional precipitation responses associated with modern interannual variability in ITCZ position. Green contours show annually averaged precipitation rates (contour interval 4 mm/day), and the black line shows the mean P_{CENT} calculated at each degree of longitude. Red and blue lines show the response of the local P_{CENT} to a 1° northward or southward shift in zonally averaged P_{CENT}, respectively. Colored shading shows the precipitation response associated with a 1° northward shift in zonally averaged P_{CENT}. Precipitation data are from the National Oceanographic and Atmospheric Administration's Climate Prediction Center's (NOAA CPC) merged analysis (Xie and Arkin, 1996) and are taken from 1981 to 2010. Core sites used for SST reconstructions are shown in numbered circles; numbers correspond to site numbers in Table 1. Sites for proxy precipitation reconstructions shown in Fig. 1 are indicated by squares with inscribed X. (For interpretation of the references to color in this figure legend, the reader is referred to the web version of this article.)

Table 1
Locations and SST proxy information for cores used for SST gradient reconstruction. Site numbers are used to show core locations in Fig. 2. References for the records are given in Shakun et al. (2012).

Site	Basin	Core	Region	SST proxy	Lat. (°N)	Long. (°E)
1	N Atlantic	MD02-2575	Gulf of Mexico	Mg/Ca	29.0	−87.1
2		M35003-4	Western tropical N Atl.	UK′37	12.1	−61.3
3		PL07-39PC	Cariaco Basin, Venezuela	Mg/Ca	10.7	−65.0
4		MD03-2707	Gulf of Guinea	Mg/Ca	2.5	9.4
5		GeoB 4905	Eastern equatorial Atl.	Mg/Ca	2.5	9.4
6	S Atlantic	GeoB 3910	Brazilian margin	UK′37	−4.2	−36.3
7		GeoB 3129	Western trop. Atl.	Mg/Ca	−4.6	−36.6
8		GeoB 6518-1	Gulf of Guinea	UK′37	−5.6	11.2
9		GeoB 1023-5	Southeast Atl.	UK′37	−17.2	11.0
10		ODP 1084B	Subtropical SE Atl.	Mg/Ca	−25.5	13.0
11	N Pacific	17940	South China Sea	UK′37	20.1	117.4
12		MD02-2529	Eastern equatorial Pac.	UK′37	8.2	−84.1
13		ME0005A-43JC	Eastern equatorial Pac.	Mg/Ca	7.9	−83.6
14		MD01-2390	South China Sea	Mg/Ca	6.6	113.4
15		MD98-2181	West Pac. warm pool	Mg/Ca	6.3	125.8
16		TR163-22	Eastern equatorial Pac.	Mg/Ca	0.5	−92.4
17	S Pacific	V21-30	Eastern equatorial Pac.	Mg/Ca	−1.2	−89.7
18		V19-28	Eastern equatorial Pac.	UK′37	−2.4	−84.7
19		MD9821-62	West Pac. warm pool	Mg/Ca	−4.7	117.9
20		MD98-2176	West Pac. warm pool	Mg/Ca	−5.0	133.4
21		MD98-2165	West Pac. warm pool	Mg/Ca	−9.7	118.4
22		MD98-2170	West Pac. warm pool	Mg/Ca	−10.6	125.4
23		MD01-2378	Timor Sea, Indian Oc.	Mg/Ca	−13.1	121.8

transports ~2.5 PW of heat into the winter hemisphere, and the magnitude of this seasonal AHT_{EQ} is linearly related to how far the ITCZ – located near the boundary between the Hadley cells – migrates into the summer hemisphere (Fig. 3A) (Donohoe et al., 2013). The ITCZ's mean position north of the equator results in an annual mean AHT_{EQ} from the northern to the southern hemisphere of approximately 0.2 PW – a small residual of the annual cycle (Trenberth and Caron, 2001).

The magnitude and direction of AHT_{EQ} are an integral part of hemispheric energy budgets, as annual mean export of heat from the NH atmosphere must be balanced by a hemispheric asymmetry in atmospheric heating, either by way of energy fluxes at the top of the atmosphere (TOA) (i.e., the balance of incoming and outgoing radiation) or surface energy fluxes resulting from ocean heat transport convergence. In the modern climate, hemispheric albedos are nearly symmetric (Marshall et al., 2013;

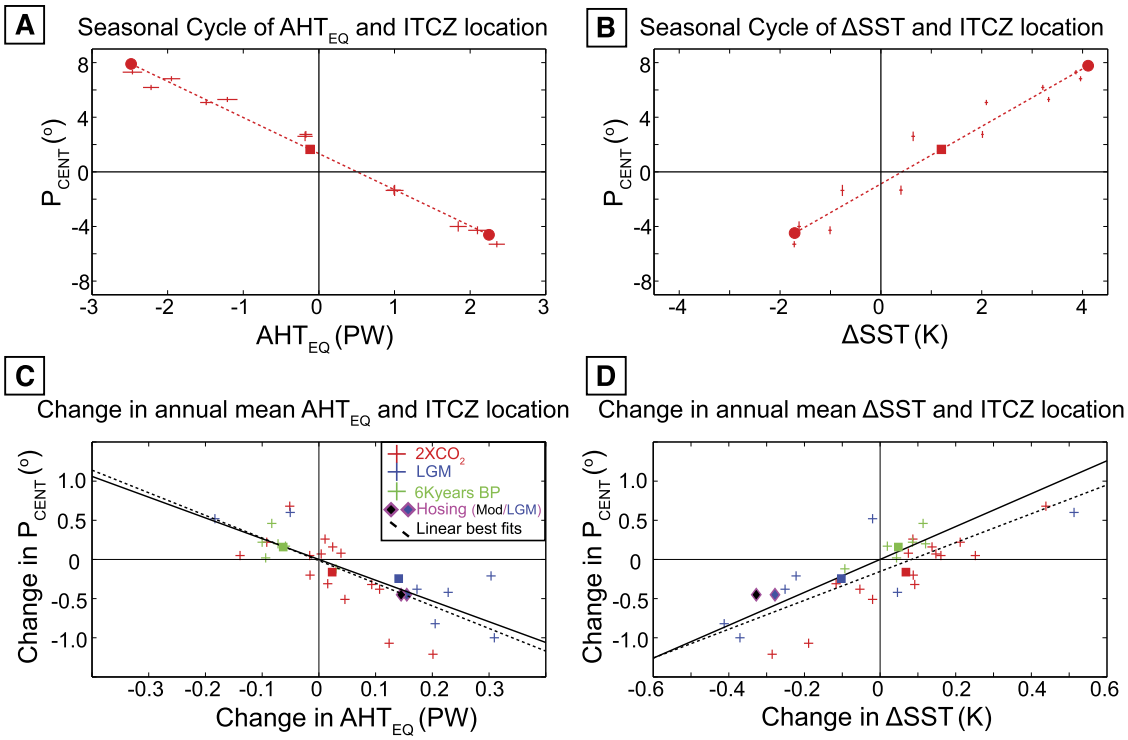

Fig. 3. Relationships between tropical SST gradients, ITCZ position and cross-equatorial AHT in the modern seasonal cycle and in models of altered climate states. (A) Relationship between ITCZ position (P_{CENT}) and cross-equatorial AHT (AHT_{EQ}) in the modern seasonal cycle (crosses: monthly averages with 95% confidence intervals based on interannual variability; dashed line: slope shows regression of monthly data, and endpoints show the amplitude of the annual harmonic; square: annual average). (B) Relationship between tropical cross-equatorial SST gradients (ΔSST) and ITCZ position in the modern seasonal cycle. (C) Relationship between P_{CENT} and cross-equatorial AHT in models of altered climates. Crosses indicate results from individual models ($2XCO_2$: doubled CO_2, red; LGM: blue; 6 ka: green; hosing experiments performed on modern and LGM background states: diamonds). Dashed line is the best linear fit to the model results, and the solid line shows the slope from the seasonal data in panel A. (D) Relationship between tropical SST gradients and ITCZ position in models of altered climates, with model symbols and lines as in C. For a list of models included in panels C and D, see Donohoe et al. (2013). (For interpretation of the references to color in this figure legend, the reader is referred to the web version of this article.)

Voigt et al., 2013) – meaning that absorbed solar radiation is approximately equal in both hemispheres – and the hemispheric asymmetry in outgoing longwave radiation is small and favors a relative cooling of the NH. These observations make clear that TOA energy fluxes are not the source of the heat exported from the NH atmosphere to the SH. Rather, the ITCZ's position in the Northern Hemisphere and the associated southward AHT_{EQ} is driven by the cross-equatorial ocean heat transport (OHT_{EQ}), which has a magnitude of ~0.4 PW and is principally driven by the Atlantic Ocean's meridional overturning circulation (AMOC) (Frierson et al., 2013; Marshall et al., 2013). Changes in ITCZ position, and thus in AHT_{EQ}, may therefore provide insight into past changes in heat transport by the AMOC; alternatively, they may reflect changes in the hemispheric balance of TOA energy fluxes (e.g., asymmetries in hemispheric albedo).

The relationship between ITCZ position and hemispheric energy budgets provides additional motivation for seeking quantitative estimates of past ITCZ shifts. Returning to HS1 as an example, a southward shift of the ITCZ during HS1 would increase AHT into the NH, compensating for a reduction or shutdown of the AMOC (Vellinga and Wu, 2008). Such compensation would provide an important conceptual basis for understanding atmospheric responses to past changes in ocean circulation. However, we have no estimates of whether the change in AHT_{EQ} during HS1 was of sufficient magnitude to compensate for the suggested reduction in northward OHT_{EQ}.

Here we present estimates of changes in the mean position of the ITCZ and cross-equatorial AHT in past climates. In Section 2 we summarize recent work that demonstrates close relationships between ITCZ position, AHT_{EQ} and tropical SST gradients in the modern seasonal cycle and in models of altered climate states (Donohoe et al., 2013), providing a means for using past SST gradients to reconstruct changes in ITCZ position and AHT_{EQ}. In Section 3 we apply these relationships to estimate globally averaged ITCZ shifts and changes in AHT_{EQ} associated with the Last Glacial Maximum (LGM; 19–23 ka), HS1, and mid-Holocene. We then explore implications of our results in Section 4, including discussion of the magnitude of past AMOC changes suggested by our findings and a consideration of the apparent mismatch between small mean ITCZ shifts suggested by our results and large precipitation changes indicated by paleo-records. Though the precision of our results is limited by the small number of tropical SST reconstructions available for these time slices, they are sufficient to define upper limits for past ITCZ shifts and changes in AHT_{EQ}, and they lay the groundwork for linking paleo-SST records to tropical precipitation patterns and hemispheric energy budgets.

2. Relationships between ITCZ position, cross-equatorial heat transport and tropical SST gradients

The ITCZ migrates north and south following the sun in the annual seasonal cycle. This migration transports heat from the warm hemisphere into the cold hemisphere via the Hadley circulation, compensating (along with heat released from the ocean) for the deficit of incoming solar radiation relative to outgoing longwave radiation in the cold hemisphere. We approximate the ITCZ's location with the tropical precipitation centroid (P_{CENT}), defined as the median latitude of zonally averaged precipitation between 20°N and 20°S (Donohoe et al., 2013; Frierson and Hwang, 2012). Using modern observational data, Donohoe et al. (2013) have demonstrated that P_{CENT} maintains a constant linear relationship with AHT_{EQ} in the seasonal cycle (Fig. 3A). The slope of the

P_{CENT}–AHT_{EQ} regression is $-2.7 \pm 0.6\,^{\circ}$/PW (95% confidence interval), meaning that 1 PW of heat is transported northward across the equator for each 2.7 degrees that P_{CENT} moves south.

P_{CENT} also has a linear relationship with the tropical cross-equatorial SST gradient in the modern seasonal cycle, with a slope of $3.3 \pm 0.6\,^{\circ}$/K ($r^2 = 0.94$; Fig. 3B) (Donohoe et al., 2013). Tropical SST gradients are linearly related to AHT_{EQ} as well, with a slope of $-1.3(\pm 0.4)$ K/PW ($r^2 = 0.93$; not shown). Here the tropical SST gradient is calculated as the average SST between 0 and 30°N minus the average SST between 30°S and 0. Note that in Donohoe et al. (2013) tropical SST gradients were calculated for the band 20°S–20°N; we use an expanded latitudinal range in order to maximize the number of cores used for reconstructions of past SST gradients.

Simulations of the preindustrial climate by the 25 coupled atmosphere–ocean general circulation models included in the Coupled Model Intercomparison Project phase 3 (CMIP3) (Meehl et al., 2007) reproduce within uncertainty the amplitude of the seasonal cycles in P_{CENT}, AHT_{EQ} and tropical SST gradients as well as the slopes of the modern seasonal P_{CENT}–AHT_{EQ}–SST relationships (Donohoe et al., 2013). The relationship of P_{CENT} and tropical SST gradients over the seasonal cycle in preindustrial runs in CMIP3 models averages $3.7 \pm 0.7\,^{\circ}$/K, in agreement with modern observations. This agreement suggests that the models' representations of the Hadley circulation and tropical precipitation and temperature patterns are robust with respect to these indices, at least in climates similar to modern.

As a test of whether the relationships between P_{CENT}, AHT_{EQ} and SST gradients would remain constant in different climates, Donohoe et al. (2013) examined the annual mean change in these parameters in model simulations of other climate states. Annual mean values for P_{CENT}, AHT_{EQ} and tropical SST gradients were calculated in simulations of the climate with atmospheric pCO_2 set at 560 ppmv (2XCO2) by CMIP3 models (Meehl et al., 2007) and simulations of the LGM and mid-Holocene (6 ka) climates included in the Paleoclimate Model Intercomparison Project phase 2 (PMIP2) (Braconnot et al., 2007a). Here we add results from two "hosing" experiments using the Community Climate System Model version 3 (CCSM3) in which freshwater perturbations are introduced to the high latitude North Atlantic ocean in modern and LGM background climate states (Bitz et al., 2007). Results were calculated by averaging the first twenty years following the freshwater pulse.

Though individual models produce quite different changes in P_{CENT} for a given set of boundary conditions – indeed, there is disagreement even as to the sign of the P_{CENT} change in the LGM, 6 ka and 2XCO2 climate states – the relationships of P_{CENT} with AHT_{EQ} and SST gradients remain close to those observed in the modern seasonal cycle. Grouping models by climate state, regression coefficients between P_{CENT} and AHT_{EQ} for the annual mean results are $-4.2\,^{\circ}$/PW for the 2XCO2 simulations, $-3.2\,^{\circ}$/PW for the LGM and 6 ka runs, and $-3.0\,^{\circ}$/PW for the hosing experiments (Fig. 3C).

Taking all the models together, the mean slope is $-3.2\,^{\circ}$/PW, within uncertainty of the modern seasonal relationship ($-2.7 \pm 0.6\,^{\circ}$/PW). This result suggests that the relationship between P_{CENT} and AHT_{EQ} observed in the modern seasonal cycle appears to be maintained in the annual mean response in different climate states. Changes in P_{CENT} and tropical SST gradients also remain linked across climates in the annual mean, though with a shallower slope than in the modern seasonal cycle, ranging from $1.5\,^{\circ}$/K in the LGM to $2.5\,^{\circ}$/K in the 2XCO2 runs; the average for all runs is $1.8\,^{\circ}$/K (Fig. 3D). The fact that models of past climates exhibit a lower sensitivity of ITCZ position to changes in tropical SST gradients suggests that using the slope observed in the modern seasonal cycle ($3.3 \pm 0.6\,^{\circ}$/K) is likely to provide an upper bound for the magnitude of past ITCZ shifts.

The importance of these results lies in the fact that tropical SST gradients for past climates can be reconstructed with greater certainty than can ITCZ position or AHT_{EQ}. With estimates of past tropical SST gradients, we can use the relationships above to estimate past changes in ITCZ position, offering insight into the zonal-mean sensitivity of tropical precipitation to climate forcings. The same relationships also allow us to estimate changes in AHT_{EQ} that point to changes in hemispheric energy budgets and OHT_{EQ} driven by the AMOC (Marshall et al., 2013).

3. Estimates of ITCZ position and cross-equatorial heat transport for past climates

3.1. Reconstruction of past tropical SST gradients

We used high resolution SST records compiled by Shakun et al. (2012) to estimate tropical cross-equatorial SST gradients for the LGM, HS1, and 6 ka climates. The dataset includes data from a total of 23 sediment cores located between 30°N and 30°S in the Pacific and Atlantic basins and the Indian Ocean portion of the West Pacific Warm Pool (Table 1; Fig. 2). The western Indian Ocean/Arabian Sea region is left out because of poor coverage south of the equator. All SST estimates are based on Mg/Ca ratios in planktonic foraminifera or alkenone paleothermometry. One tropical core included in Shakun et al. (2012) is left out because it is located on the equator. All gradients are normalized to the cross-equatorial gradient observed between 0 and 2 ka in these cores; cores without 0–2 ka data were not included. Time slices are defined as: LGM, 19–23 ka; HS1, 15.5–17.5 ka; and 6 ka, 6–8 ka.

We use a jackknifing procedure to estimate uncertainties. We first generated 1000 realizations of each core's temperature in each time interval by randomly sampling within the uncertainty estimate of the mean temperature for the interval. Random uncertainties in proxy data and proxy calibrations are assumed to be contained within the scatter of data during each time interval and to be represented by the standard error of the mean. For each of these 1000 realizations, temperatures for the 6 ka, HS1 and LGM time slices were differenced from 0 to 2 ka temperatures (ΔT). Within each realization, we then randomly selected all cores but one in each hemisphere of the Pacific and Atlantic basin in order to estimate the impact of the limited number of cores on our temperature gradient estimates. Basin-average ΔT values for the sampled cores were then differenced by hemisphere to obtain 1000 estimates of the Pacific and Atlantic cross-equatorial SST gradients, and these values were multiplied by the relative width of each basin and summed to generate a combined SST gradient. The standard deviation of these 1000 realizations is used as an estimate of the uncertainty of this procedure.

Past changes in global mean ITCZ position and AHT_{EQ} are calculated using the above estimates of past tropical SST gradients and the SST–P_{CENT}–AHT_{EQ} relationships observed in the modern seasonal cycle. Stated uncertainties include uncertainties in past SST gradients and in the seasonal SST–P_{CENT} and SST–AHT_{EQ} relationships. Uncertainties dominantly reflect the small number of cores. While development of additional SST records will improve the precision of these estimates, our results are sufficient to place upper bounds on past changes in ITCZ position and AHT_{EQ}.

3.2. ITCZ position and cross-equatorial AHT during LGM, HS1 and 6 ka climates

We estimate that the LGM tropical cross-equatorial SST gradient relative to 0–2 ka was -0.14 ± 0.18 K (68% confidence interval) (Table 2). Negative values indicate colder temperatures in the NH

Table 2
Estimates of changes in cross-equatorial tropical SST gradients, P_{CENT} and cross-equatorial AHT at 6 ka, HS1 and the LGM. SST gradients are calculated from proxy data, and P_{CENT} and AHT changes are derived from seasonal slopes; see text for details. Multi-model mean values from the CMIP3 doubled-CO_2 runs are also shown for comparison. 68% confidence intervals are given.

Time slice	Change in SST gradient (°C)	Change in P_{CENT} (°)	Change in cross-equatorial AHT (PW)
6 ka	+0.12 (±0.18)	+0.25 (±0.38)	−0.09 (±0.14)
HS1	−0.29 (±0.22)	−0.61 (±0.47)	+0.22 (±0.18)
LGM	−0.14 (±0.18)	−0.29 (±0.38)	+0.11 (±0.14)
2XCO2	−0.07 (±0.18)	−0.16 (±0.50)	+0.02 (±0.09)

tropics. This result is similar to that obtained from the gridded LGM SST product from the MARGO project of −0.11 K (Waelbroeck et al., 2009), suggesting that our use of high-accumulation rate sites does not significantly bias our result. As not all MARGO cores have 0–2 ka data, the LGM SST gradient for these data is expressed as a deviation from the modern observed (World Ocean Atlas) SST gradient, following MARGO conventions (Waelbroeck et al., 2009).

Using the relationships observed in the modern seasonal cycle, this change in SST gradient corresponds to a $-0.29 \pm 0.38°$ shift in the ITCZ at the LGM and a 0.11 ± 0.14 PW increase in AHT_{EQ} into the Northern Hemisphere relative to the last 2 ka.

During HS1, these cores suggest a change in tropical SST gradients of -0.29 ± 0.22 K relative to modern. This change implies a mean ITCZ shift of $-0.61 \pm 0.47°$ and an increase in northward AHT_{EQ} of 0.22 ± 0.18 PW. At 6 ka, we estimate a change in tropical SST gradients of $+0.12 \pm 0.18$ K, suggesting a northward movement of the ITCZ's mean position of $0.25 \pm 0.38°$ and a change in AHT_{EQ} of -0.09 ± 0.14 PW.

4. Discussion

4.1. Evaluation of estimated SST gradient and ITCZ position changes

Tropical SST gradient changes during the LGM, HS1, and 6 ka climates reconstructed using published data have large uncertainties due to the small number of records available. However, the sign and relative magnitudes of mean values for SST gradient changes compare well to more robust estimates of whole-hemisphere temperature gradient changes (Fig. 4) (Shakun et al., 2012; Marcott et al., 2013). Additionally, the LGM gradient is similar to that estimated from a larger number of cores in the MARGO project (Waelbroeck et al., 2009). This agreement suggests that the median values are of reasonable magnitude and the correct sign.

Despite their large uncertainties, these data are sufficient to provide upper bounds on past shifts in the ITCZ's mean position. The data suggest a small southward shift of P_{CENT} during the LGM, with a median estimate of only ∼35 km, and <5% probability that the mean shift was greater than 1° south.

The data suggest a larger southward shift in mean ITCZ position during HS1, with a median estimate of −0.6°, but there is still only ∼20% probability that the shift was greater than 1° south. The direction of this shift is consistent with a wide range of paleo-data. Sites in the northern tropics consistently record drier conditions during HS1 (e.g., Escobar et al., 2012; Peterson et al., 2000; Rashid et al., 2011; Wang et al., 2001), and several sites in the southern tropics record wetter conditions at this time (Cruz et al., 2005; Denniston et al., 2013; Kanner et al., 2012; Muller et al., 2008; Placzek et al., 2006; Wang et al., 2004) (Fig. 1).

At 6 ka, the data suggest that a small northward shift in mean ITCZ position is likely (+0.3°), consistent with data suggesting wetter conditions in the northern tropics (Adkins et al., 2006; Dykoski et al., 2005; Fleitmann et al., 2007; Gasse, 2000; Haug et al., 2001; Weldeab et al., 2007) and a weaker South American summer monsoon (Cruz et al., 2005; Seltzer et al., 2000) (Fig. 1).

4.2. Past changes in cross-equatorial heat transport

Though the changes in P_{CENT} in past climates appear to have been small in the zonal mean, the implied AHT_{EQ} changes may have been substantial with respect to the modern value of approximately −0.2 PW (negative values indicate heat transport toward the south). Any change in AHT_{EQ} must be accompanied by a change in the hemispheric asymmetry of atmospheric heating either by way of (a) a change in heat fluxed from the ocean – which over multi-decadal timescales should reflect a change in cross-equatorial ocean heat transport, likely due to a change in the AMOC – or (b) a change in net radiation at the top of the atmosphere, for instance due to a change in that hemisphere's surface or cloud albedo. (We assume that changes in the hemispheric asymmetry of energy storage in the atmosphere are negligible.) In the discussion below we will consider the roles of each of these processes in driving changes in AHT_{EQ} during the LGM, HS1 and 6 ka time slices.

Our estimates suggest that an increase in northward AHT_{EQ} across the equator at the LGM is likely (0.11 ± 0.14 PW). In models simulating LGM climate, this change is driven by the larger increase in albedo in the NH relative to the SH at the LGM (for a discussion of LGM energy balance, see Donohoe et al., 2013). A slight decrease in OHT_{EQ} due to reduced volume transport by the AMOC is also a possible contributor to the increase in northward AHT_{EQ}. As modern OHT_{EQ} is ∼0.4 PW, a ∼25% decrease in the AMOC could drive a 0.1 PW decrease in AHT_{EQ}. Pa/Th data from the Bermuda Rise suggest a slight reduction in AMOC intensity at the LGM relative to the Holocene (Fig. 4) (McManus et al., 2004), and South Atlantic benthic $\delta^{18}O$ data are also consistent with a reduction (Lynch-Stieglitz et al., 2006). However, recent inverse modeling studies using Pa/Th (Lippold et al., 2012) and SST and air temperature data (Ritz et al., 2013) suggest no difference in AMOC strength between the LGM and the Holocene.

A larger increase in northward AHT_{EQ} is likely during HS1; our estimates indicate that this change (0.22 ± 0.18 PW) may have been a substantial fraction of modern cross-equatorial ocean heat transport, which is primarily driven by the AMOC and is approximately 0.4 PW (Ganachaud and Wunsch, 2000). Examination of heat transports in the hosing experiments suggest nearly complete compensation by AHT_{EQ} for changes in OHT_{EQ}; in both experiments, northward OHT_{EQ} decreases substantially as the AMOC weakens following the hosing, but northward AHT_{EQ} increases by almost the same magnitude in association with the southward shift of the mean ITCZ, resulting in only a small reduction in total heat transport into the NH (Fig. 5, top).

This compensation suggests that our reconstructed AHT_{EQ} changes may provide insight into the magnitude of changes in OHT_{EQ} by the AMOC at HS1. Pa/Th data point to a substantial reduction of AMOC strength during HS1 (McManus et al., 2004), and $\delta^{13}C$ and Cd/Ca data suggest large changes in water mass properties consistent with reduced production of northern-sourced deep waters (Boyle and Keigwin, 1987). Supporting these inferences, inverse modeling of SST and air temperature data with an intermediate-complexity model indicates a 25–100% reduction in AMOC at HS1 (Ritz et al., 2013). Uncertainty remains, however, over the duration and magnitude of AMOC weakening; radiocarbon data from benthic foraminifera, shells and deep-sea corals do not suggest as long-lived a change in the AMOC (Robinson et al., 2005; Keigwin and Boyle, 2008), and low $\delta^{13}C$ values in North Atlantic benthic foraminifera during HS1 may reflect waters derived from North Atlantic brine rejection rather than southern sources (Thornalley et al., 2010). As the AHT_{EQ} change we reconstruct at

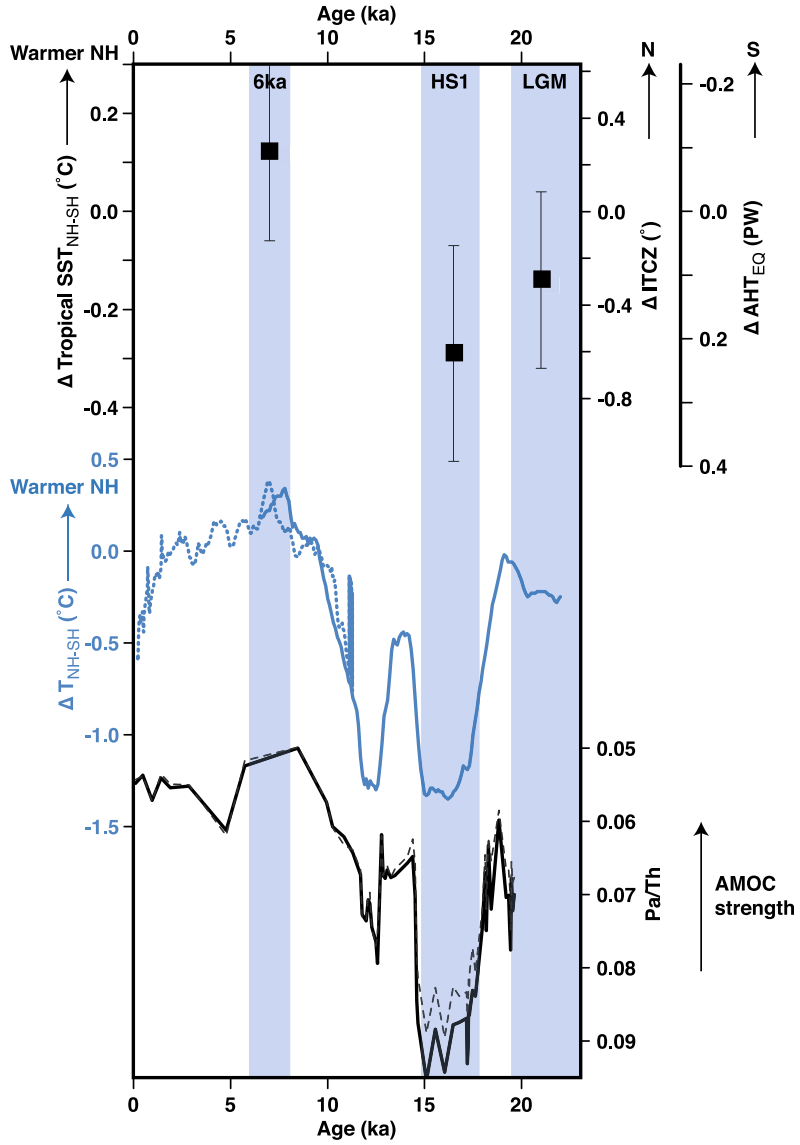

Fig. 4. Past changes in tropical SST gradients, ITCZ position and cross-equatorial heat transport. (Top) Estimates from this study for the mid-Holocene (6 ka) Heinrich Stadial 1 (HS1), and Last Glacial Maximum (LGM), shown plotted against axes showing changes cross-equatorial tropical SST gradients (ΔTropical SST$_{NH-SH}$), mean ITCZ location (ΔITCZ) and cross-equatorial AHT (ΔAHT$_{EQ}$) relative to present. Values near the top of the figure indicate warmer SSTs in the NH tropics, northward displacement of the ITCZ, and southward AHT, respectively. Error bars express 68% confidence interval for SST gradients. (Middle) Reconstructions of whole-hemisphere surface temperature gradients expressed as the area-weighted mean NH surface temperature minus SH surface temperature; values are relative to the 11–6.5 ka mean for each record (solid: Shakun et al., 2012; dashed: Marcott et al., 2013). (Bottom) Unsupported ^{231}Pa/^{230}Th data from Bermuda Rise site OCE326-GGC5, interpreted as primarily reflecting variations in the volume transport by the AMOC (McManus et al., 2004), and used here as an indicator of changes in cross-equatorial ocean heat transport. Calculations of unsupported fractions of Pa and Th are shown based on ^{238}U (solid) and ^{232}Th (dashed) concentrations.

HS1 is a large fraction of the magnitude of modern cross-equatorial OHT$_{EQ}$, our results are consistent with a substantial reduction of northward heat transport by the AMOC during HS1, which then led to a compensating change in AHT$_{EQ}$ through a southward mean ITCZ shift.

At 6 ka, our estimates suggest that an increase in AHT$_{EQ}$ into the SH is likely (-0.09 ± 0.14 PW). Braconnot et al. (2007b) relate the northward displacement of the mean ITCZ at 6 ka to (a) warming of the tropical North Atlantic ocean and (b) reduced NH albedo due to increased vegetation density in subtropical regions and melting of NH sea ice and snow during boreal summer. Each of these changes is a consequence of higher NH summer insolation than at present. If a decrease in NH surface albedo was not canceled by cloud albedo changes, AHT$_{EQ}$ into the SH would have increased in order to achieve a near-balance in outgoing longwave radiation between the hemispheres. In addition, a small mid-Holocene increase in OHT$_{EQ}$ into the NH cannot be ruled out as contributing to the increase in southward AHT$_{EQ}$; changes in important components of North Atlantic Deep Water between the mid-Holocene and modern are suggested by some (but not all) proxy records (Kissel et al., 2013).

As AHT$_{EQ}$ changes at the rate of ~1 PW for every 3 degrees north–south shift in the ITCZ, P_{CENT} shifts of more than a degree of latitude require either large changes in hemispheric heat budgets (e.g., very large changes in the AMOC or in the hemispheric albedo asymmetry) or a fundamental change in the intensification of the winter Hadley cell as the ITCZ moves away from the equator (which determines the P_{CENT}–AHT$_{EQ}$ relationship; Donohoe et al., 2013). This proportionality places an important energetic constraint on past changes in mean ITCZ position. If AHT$_{EQ}$ is primarily responding to changes in OHT$_{EQ}$ (Frierson et al., 2013; Marshall et al., 2013), a southward shift of the mean ITCZ by

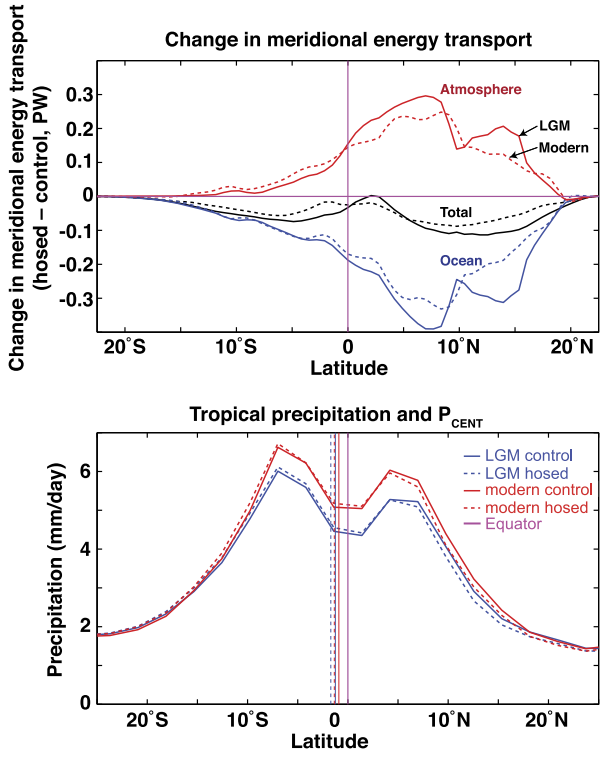

Fig. 5. Changes in heat transport and tropical precipitation in two hosing experiments. (Top) Changes in meridional heat transport in the first 20 years of hosing of LGM and modern background climates using the CCSM3 model (Bitz et al., 2007). Note the nearly complete compensation of atmospheric heat transport for changes in ocean heat transport. Dashed lines: Hosing results for modern background climate; Solid lines: hosing results for LGM climate; Black: Total (ocean + atmosphere) meridional heat transport; Red: Atmospheric heat transport; Blue: ocean heat transport. (Bottom) Zonally averaged precipitation in control (solid) and hosing (dashed) experiments based on modern (red) and LGM (blue) climate states using CCSM3. Vertical lines show P_{CENT} for each model run. Note the minimal differences in the zonally averaged precipitation between control and hosing runs for each climate state, suggesting that regional precipitation responses are much larger than the zonal mean response. (For interpretation of the references to color in this figure legend, the reader is referred to the web version of this article.)

more than 1.5° would require a reversal of the ocean's heat transport. Reconstructions estimating large regional shifts – for example, a 5° southward shift of the central Pacific ITCZ in Little Ice Age (Sachs et al., 2009), a 7° southward shift of the Atlantic ITCZ at the LGM and a 7° northward shift during the early Holocene (Arbuszewski et al., 2013), and a >10° northward shift of the Pacific ITCZ in the Miocene (Hyeong et al., 2005; Kim et al., 2006; Lyle et al., 2002) – must therefore reflect changes occurring over <15–20% of the globe, with minimal changes at all other longitudes. As described in Section 4.3, these proxy records thus point to important regional-scale precipitation changes, but extension of these estimates beyond limited regions would lead to unrealistic changes in hemispheric heat budgets.

4.3. Implications for past changes in tropical precipitation: regional and seasonal differences in ITCZ responses

The tropical proxy records cited above and plotted in Fig. 1 indicate large changes in local summer precipitation and precipitation–evaporation (P–E) during past climates. Our work places a constraint on past ITCZ changes, as we find that changes in the ITCZ's annually and zonally averaged position during LGM, HS1 and 6 ka climates were small – likely a degree of latitude or less.

This finding is not inconsistent with large changes in local precipitation inferred from proxy records; local responses much larger than the globally averaged response are to be expected to a given climate change. As an example, hosing experiments simulating North Atlantic cooling forced by freshwater inputs – the hypothesized trigger of the largest southward shifts in the ITCZ over the late Pleistocene – generally show the largest tropical precipitation responses in the Atlantic Ocean and eastern Pacific, with smaller and less coherent changes in the western Pacific and Indian oceans (Chiang and Friedman, 2012; Vellinga and Wood, 2002; Zhang and Delworth, 2005). This zonal variability leads to quite muted changes in the zonally averaged precipitation in model results: in the CCSM3 hosing experiments examined in this study, no latitude between 30°N and 30°S experiences more than a 10% change in precipitation (Fig. 5, bottom). Zonal heterogeneity is also suggested by proxy data: precipitation proxies suggest a relatively simple dipole response during HS1 in Central and South America, with precipitation decreasing in Central America and northern South America and increasing in South America south of the equator (Fig. 1) (e.g., Escobar et al., 2012; Peterson et al., 2000; Placzek et al., 2006; Wang et al., 2004), while tropical Africa appears to record drying both north and south of the equator (Stager et al., 2011). Recent work has also pointed out the importance of changes in zonal tropical circulation cells (e.g., the Walker circulation; DiNezio et al., 2011).

Zonal heterogeneity is also evident in modern interannual variability of ITCZ position. Fig. 2 shows the local precipitation change and P_{CENT} change associated with a 1° northward shift of P_{CENT} in modern interannual variability. While ITCZ changes in past climates are likely to be different from modern interannual changes, the plot makes clear that the scale of changes in local precipitation rates and P_{CENT} for a given global P_{CENT} change differs quite markedly in different parts of the tropics. Interestingly, the central Pacific stands out as a region of high precipitation and P_{CENT} variability in the modern climate, with P_{CENT} in this region moving ~5° for a global 1° shift. This observation suggests that large-scale changes in the position of the central Pacific ITCZ – as reconstructed for the Little Ice Age (Sachs et al., 2009) and for the Miocene (Hyeong et al., 2005; Kim et al., 2006; Lyle et al., 2002) – may be plausible, but changes in the position of the globally averaged ITCZ are likely to be much smaller.

Seasonality also plays a large role in determining local precipitation responses to mean ITCZ shifts. In the annual cycle, the ITCZ spends most of its time near its summer positions in the two hemispheres and relatively little time near its mean position (Fig. 6, left-hand panels of B–D). It is thus important to ask whether past mean ITCZ shifts were marked by changes in the position of only one seasonal extreme, changes in the position of both extremes, changes in the amount of time spent by the ITCZ near each extreme, or changes in the intensity of precipitation at one or both extremes; all of these changes would lead to a change in zonal mean ITCZ position, but each would impact precipitation at individual sites differently.

Model results provide one perspective on past changes in ITCZ seasonality. Here we examine results from the Simulation of Transient Climate Evolution over the last 21,000 ka (TraCE-21 ka) experiment using CCSM3 (He, 2011; Liu et al., 2009). The relationships between P_{CENT}, AHT_{EQ} and tropical SST gradients in this simulation are consistent within uncertainty with those seen in the model results in Fig. 3. In this experiment's simulation of the last 21 ka, important differences emerge in the seasonal response of the ITCZ to past climate changes (Fig. 6, left-hand panels of B–D). At the LGM, the ITCZ's zonal-mean SH summer position is shifted ~1° south relative to the modern climate in the model, while the NH summer position experiences a much smaller southward shift. A similar pattern is observed in the LGM simulation in the IPSL model (Fig. 11 in Donohoe et al., 2013). During HS1, both seasonal positions shift south by approximately 1–1.5° relative to the modern, consistent with the opposite precipitation responses recorded

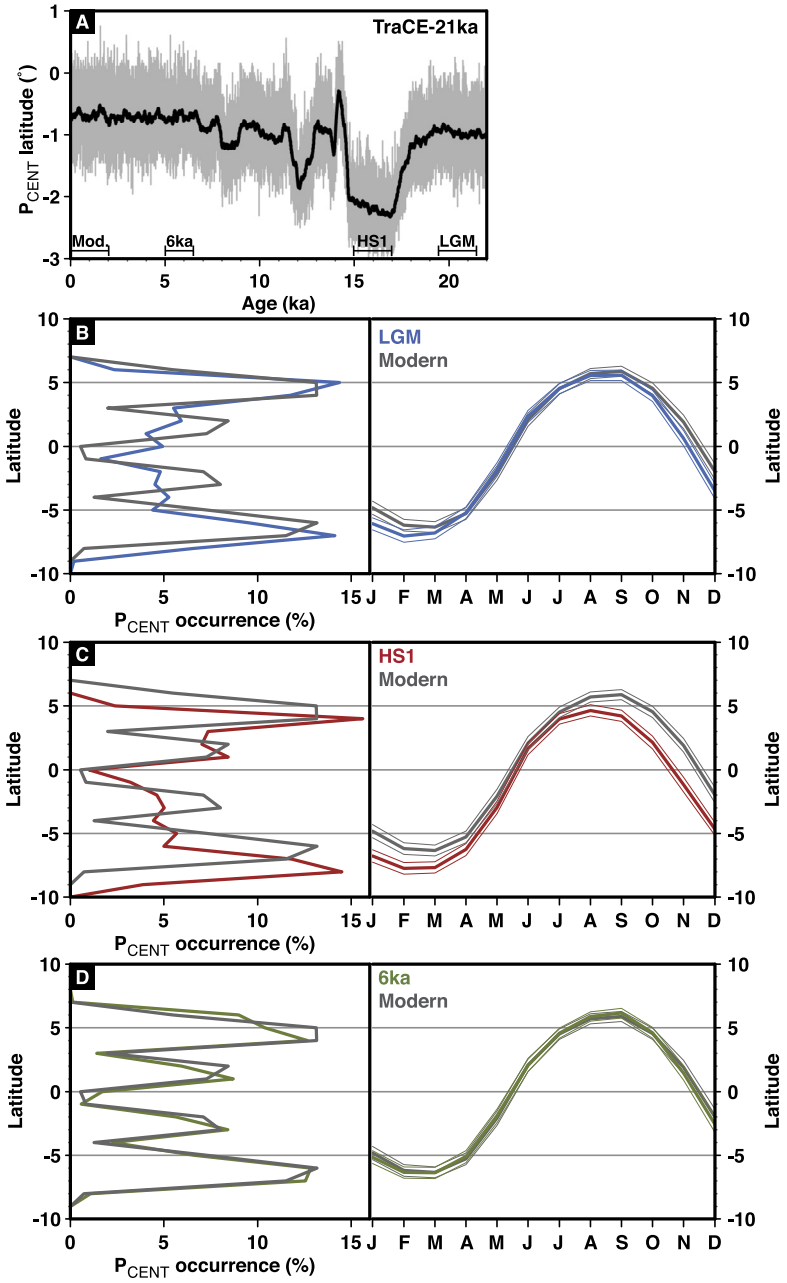

Fig. 6. Changes in mean ITCZ position and seasonal ITCZ migration in the TraCE-21 ka simulation. (A) Mean P_{CENT} position in the simulation through the last 21 ka. Annual averages are shown in grey, and a 100-year running mean is shown in black. Time slices plotted in bottom panels are indicated at the bottom of the figure. (B)–(D) In the left panels, histograms of P_{CENT} location are shown for the LGM, HS1 and 6 ka time slices, respectively, each plotted against the histogram for the modern time slice; values reflect the average percent of time spent by P_{CENT} at each degree latitude. In the right panels, average P_{CENT} positions are plotted for each month of the year for each time slice, again plotted against the modern. Thin lines indicate ±1 standard deviation. The left panels show changes in the seasonal positions of the ITCZ between the time slices, and the right panels show changes in the amount of time spent in each hemisphere, with the ITCZ moving into the SH earlier in the fall in both the LGM and HS1 time slices.

by tropical proxy data north and south of the equator in South America and in Asia and Indo-Australia (Fig. 1) (Ayliffe et al., 2013; Denniston et al., 2013; Peterson et al., 2000; Placzek et al., 2006; Rashid et al., 2011; Wang et al., 2007). At 6 ka, the NH summer position shifts slightly north while no change is observed in the SH summer position; this seasonal response is again similar to that observed in the IPSL model (Donohoe et al., 2013).

The model also indicates changes in the amount of time that the ITCZ spends in each hemisphere (Fig. 6, right-hand panels of B–D). Relative to the last 2 ka of the model run, the ITCZ spends 2% less time in the NH during the LGM time slice, 9% less time during HS1, and very slightly (0.1%) more time during the mid-Holocene. In HS1, the migration of the ITCZ into the SH occurs ~1 month earlier in the fall than in the modern (0–2 ka) time slice. The relative intensity of precipitation near each seasonal extreme does not change substantially (not shown). The latitudinal range of seasonal ITCZ migration shows only modest changes in the TraCE-21 ka results, with a slight stretching of its range at the LGM and 6 ka relative to the modern.

These seasonal differences in ITCZ response and the mismatch between large local responses in proxy records and small changes in the mean ITCZ only increase the importance of proxy records in documenting responses to past climate changes. Because modern observations, proxy data from well-documented

time slices in the past, and model output all indicate that changes in tropical precipitation are characterized by regionally and seasonally variable responses rather than zonally consistent, seasonally symmetric shifts, a high density of records is required to adequately determine the impact of various forcings on tropical precipitation patterns. A corollary of this observation is that proxy records from a given region of the tropics primarily reflect local changes in precipitation patterns rather than global ITCZ shifts.

5. Conclusions

Recent work demonstrates strong connections between tropical cross-equatorial SST gradients, zonal-mean ITCZ position and cross-equatorial AHT in the modern seasonal cycle that appear to remain stable in annual mean changes in simulations of altered climates (Donohoe et al., 2013). Applying these relationships, we use reconstructions of past tropical SST gradients to estimate changes in mean ITCZ position and cross-equatorial AHT at the LGM, HS1 and 6 ka. There is substantial uncertainty in past tropical SST gradients due to the small number of cores available, but the sign and relative magnitude of the median reconstructed changes is consistent with more robust reconstructions of whole-hemisphere cross-equatorial temperature gradients for each time slice (Marcott et al., 2013; Shakun et al., 2012). We find that past changes in annual- and zonal-mean ITCZ position are likely to have been small, with mean changes for each time slice a maximum of 0.6° different from the modern position and small likelihood of changes greater than 1° latitude.

Comparison of these small mean ITCZ changes with proxy evidence for large-scale precipitation changes in certain areas of the tropics during HS1 and 6 ka climates suggests that the ITCZ's response to these past climates exhibited substantial zonal and seasonal heterogeneity. This contrast reinforces the understanding that tropical precipitation proxy records should be used to characterize the regional and seasonal variability of tropical precipitation responses to different climate forcings rather than simply interpreted as reflecting global ITCZ "shifts." In addition, our findings link regional ITCZ reconstructions to ITCZ shifts elsewhere in the world, as large changes in ITCZ position inferred for specific regions place limits on changes everywhere else. As an example, a 5° meridional shift in the mean ITCZ can occur over a maximum of 70° of longitude (i.e. slightly larger than the equatorial Atlantic basin, or half the width of the equatorial Pacific), and ITCZ shifts at all other longitudes must be zero, for the global mean shift to be $\leqslant 1°$ as suggested by our analysis.

Past SST gradients allow for substantial changes in cross-equatorial AHT, with past changes potentially equaling or exceeding the estimated magnitude of modern annual-mean AHT_{EQ} (~ -0.2 PW). During HS1, we estimate that northward AHT_{EQ} increased by 0.22 ± 0.18 PW, consistent with atmospheric compensation for a large reduction in northward ocean heat transport due to a weakened AMOC. Our results also allow for a change toward more northward AHT_{EQ} during the LGM and an increase in southward AHT_{EQ} at 6 ka; these changes may relate to hemispheric differences in net radiation (for instance, due to albedo changes), or they may point to smaller changes in AMOC intensity.

The relationship between tropical SST gradients and AHT_{EQ} used by this study suggests that robust reconstructions of tropical SSTs offer a window into the energy budgets of past climates. In addition, the high sensitivity of AHT_{EQ} to small changes in mean ITCZ position ($\sim$1 PW/3° latitude) places a fundamental limit on the magnitude of past mean ITCZ shifts. Though future work utilizing models and theory will be needed to explore the stability of modern seasonal relationships for annual mean responses in different climates, this study suggests that it is difficult to accomplish multiple-degree shifts in mean ITCZ position without fundamental changes in hemispheric energy budgets.

Acknowledgements

We thank Cecilia Bitz and John Chiang for providing hosing simulation results; Jeremy Shakun and Shaun Marcott for providing temperature gradient data used in Fig. 1; and Bette Otto-Bliesner for facilitating use of the TraCE-21 ka results. Two reviewers and editor Jean Lynch-Steiglitz provided insightful input that improved the manuscript. TraCE-21 ka was made possible by the DOE INCITE computing program, and supported by NCAR, the NSF P2C2 program, and the DOE Abrupt Change and EaSM programs. A.D. is supported by a NOAA Climate and Global Change postdoctoral fellowship.

References

Adkins, J., deMenocal, P., Eshel, G., 2006. The "African humid period" and the record of marine upwelling from excess ^{230}Th in Ocean Drilling Program Hole 658C. Paleoceanography 21, PA4203. doi:4210.1029/2005PA001200.

Arbuszewski, J.A., deMenocal, P.B., Cléroux, C., Bradtmiller, L., Mix, A., 2013. Meridional shifts of the Atlantic intertropical convergence zone since the Last Glacial Maximum. Nat. Geosci. 6, 1–4. http://dx.doi.org/10.1038/ngeo1961.

Ayliffe, L.K., Gagan, M.K., Zhao, J.-X., Drysdale, R.N., Hellstrom, J.C., Hantoro, W.S., Griffiths, M.L., Scott-Gagan, H., Pierre, E.S., Cowley, J.A., Suwargadi, B.W., 2013. Rapid interhemispheric climate links via the Australasian monsoon during the last deglaciation. Nat. Commun. 4. http://dx.doi.org/10.1038/ncomms3908.

Bard, E., Rostek, F., Turon, J., Gendreau, S., 2000. Hydrological impact of Heinrich events in the subtropical northeast Atlantic. Science 289, 1321–1324.

Bitz, C.M., Chiang, J.C.H., Cheng, W., Barsugli, J.J., 2007. Rates of thermohaline recovery from freshwater pulses in modern, Last Glacial Maximum, and greenhouse warming climates. Geophys. Res. Lett. 34. http://dx.doi.org/10.1029/2006GL029237.

Boyle, E., Keigwin, L., 1987. North Atlantic thermohaline circulation during the past 20,000 years linked to high-latitude surface temperature. Nature 330, 35–40.

Braconnot, P., Otto-Bliesner, B., Harrison, S., Joussaume, S., Peterchmitt, J.-Y., Abe-Ouchi, A., Crucifix, M., Driesschaert, E., Fichefet, T., Hewitt, C., Kageyama, M., Kitoh, A., Laine, A., Loutre, M.-F., Marti, O., Merkel, U., Ramstein, G., Valdes, P., Weber, S., Yu, Y., Zhao, Y., 2007a. Results of PMIP2 coupled simulations of the mid-Holocene and Last Glacial Maximum – Part 1: experiments and large-scale features. Clim. Past 3, 261–277.

Braconnot, P., Otto-Bliesner, B., Harrison, S., Joussaume, S., Peterchmitt, J.Y., Abe-Ouchi, A., Crucifix, M., Driesschaert, E., Fichefet, T., Hewitt, C.D., Kageyama, M., Kitoh, A., Loutre, M.F., Marti, O., Merkel, U., Ramstein, G., Valdes, P., Weber, L., Yu, Y., Zhao, Y., 2007b. Results of PMIP2 coupled simulations of the mid-Holocene and Last Glacial Maximum – Part 2: feedbacks with emphasis on the location of the ITCZ and mid- and high latitudes heat budget. Clim. Past 3, 279–296.

Chiang, J., Friedman, A., 2012. Extratropical cooling, interhemispheric thermal gradients, and tropical climate change. Annu. Rev. Earth Planet. Sci. 40, 383–412.

Clark, P.U., Shakun, J.D., Baker, P.A., Bartlein, P.J., Brewer, S., Brook, E., Carlson, A.E., Cheng, H., Kaufman, D.S., Liu, Z., Marchitto, T.M., Mix, A.C., Morrill, C., Otto-Bliesner, B.L., Pahnke, K., Russell, J.M., Whitlock, C., Adkins, J.F., Blois, J.L., Clark, J., Colman, S.M., Curry, W.B., Flower, B.P., He, F., Johnson, T.C., Lynch-Stieglitz, J., Markgraf, V., McManus, J., Mitrovica, J.X., Moreno, P.I., Williams, J.W., 2012. Global climate evolution during the last deglaciation. Proc. Natl. Acad. Sci. USA 109, E1134–E1142. http://dx.doi.org/10.1073/pnas.1116619109.

Cruz Jr., F.W., Burns, S.J., Karmann, I., Sharp, W.D., Vuille, M., Cardoso, A.O., Ferrari, J.A., Silva Dias, P.L, Viana Jr., O., 2005. Insolation-driven changes in atmospheric circulation over the past 116,000 years in subtropical Brazil. Nature 434, 63–66.

Denniston, R.F., Wyrwoll, K.-H., Asmerom, Y., Polyak, V.J., Humphreys, W.F., Cugley, J., Woods, D., LaPointe, Z., Peota, J., Greaves, E., 2013. North Atlantic forcing of millennial-scale Indo-Australian monsoon dynamics during the Last Glacial period. Quat. Sci. Rev. 72, 159–168.

DiNezio, P.N., Clement, A., Vecchi, G.A., Soden, B., Broccoli, A.J., Otto-Bliesner, B.L., Braconnot, P., 2011. The response of the Walker circulation to Last Glacial Maximum forcing: Implications for detection in proxies. Paleoceanography 26. http://dx.doi.org/10.1029/2010PA002083.

Donohoe, A., Marshall, J., Ferreira, D., McGee, D., 2013. The relationship between ITCZ location and cross equatorial atmospheric heat transport; from the seasonal cycle to the last glacial maximum. J. Climate 26, 3597–3618.

Dykoski, C.A., Edwards, R.L., Cheng, H., Yuan, D.X., Cai, Y.J., Zhang, M.L., Lin, Y.S., Qing, J.M., An, Z.S., Revenaugh, J., 2005. A high-resolution, absolute-dated Holocene and deglacial Asian monsoon record from Dongge Cave, China. Earth Planet. Sci. Lett. 233, 71–86.

Escobar, J., Hodell, D.A., Brenner, M., Curtis, J.H., Gilli, A., Mueller, A.D., Anselmetti, F.S., Ariztegui, D., Grzesik, D.A., Pérez, L., Schwalb, A., Guilderson, T.P., 2012. A ~43-ka record of paleoenvironmental change in the Central American lowlands inferred from stable isotopes of lacustrine ostracods. Quat. Sci. Rev. 37, 92–104.

Fleitmann, D., Burns, S.J., Mangini, A., Mudelsee, M., Kramers, J., Villa, I., Neff, U., Al-Subbary, A.A., Buettner, A., Hippler, D., Matter, A., 2007. Holocene ITCZ and Indian monsoon dynamics recorded in stalagmites from Oman and Yemen (Socotra). Quat. Sci. Rev. 26, 170–188.

Frierson, D.M.W., Hwang, Y.T., 2012. Extratropical influence on ITCZ shifts in slab ocean simulations of global warming. J. Climate 25, 720–733.

Frierson, D.M.W., Hwang, Y.-T., Fuckar, N.S., Seager, R., Kang, S.M., Donohoe, A., Maroon, E.A., Liu, X., Battisti, D.S., 2013. Contribution of ocean overturning circulation to tropical rainfall peak in the northern hemisphere. Nat. Geosci. 6, 940–944.

Ganachaud, A., Wunsch, C., 2000. Improved estimates of global ocean circulation, heat transport and mixing from hydrographic data. Nature 408, 453–457.

Gasse, F., 2000. Hydrological changes in the African tropics since the Last Glacial Maximum. Quat. Sci. Rev. 19, 189–211.

Gibbons, F.T., Oppo, D.W., Mohtadi, M., Rosenthal, Y., Cheng, J., Liu, Z., Linsley, B.K., 2014. Deglacial $\delta^{18}O$ and hydrologic variability in the tropical Pacific and Indian Oceans. Earth Planet. Sci. Lett. 387, 240–251.

Haug, G.H., Hughen, K.A., Sigman, D.M., Peterson, L.C., Rohl, U., 2001. Southward migration of the intertropical convergence zone through the Holocene. Science 293, 1304–1308.

He, F., 2011. Simulating transient climate evolution of the last deglaciation with CCSM3. Ph.D. Dissertation. University of Wisconsin-Madison.

Hyeong, K., Park, S.-H., Yoo, C.M., Kim, K.-H., 2005. Mineralogical and geochemical compositions of the eolian dust from the northeast equatorial Pacific and their implications on paleolocation of the Intertropical Convergence Zone. Paleoceanography 20. http://dx.doi.org/10.1029/2004PA001053.

Kanner, L.C., Burns, S.J., Cheng, H., Edwards, R.L., 2012. High-latitude forcing of the South American summer monsoon during the last glacial. Science 335, 570–573.

Keigwin, L.D., Boyle, E.A., 2008. Did North Atlantic overturning halt 17,000 years ago? Paleoceanography 23, PA1101. http://dx.doi.org/10.1029/2007PA001500.

Kim, J., Hyeong, K., Jung, H.S., Moon, J.W., Kim, K.H., Lee, I., 2006. Southward shift of the Intertropical Convergence Zone in the western Pacific during the late Tertiary: Evidence from ferromanganese crusts on seamounts west of the Marshall Islands. Paleoceanography 21. http://dx.doi.org/10.1029/2006PA001291.

Kissel, C., Van Toer, A., Laj, C., Cortijo, E., Michel, E., 2013. Variations in the strength of the North Atlantic bottom water during Holocene. Earth Planet. Sci. Lett. 369–370, 248–259.

Lippold, J., Luo, Y., Francois, R., Allen, S.E., Gherardi, J., Pichat, S., Hickey, B., Schulz, H., 2012. Strength and geometry of the glacial Atlantic meridional overturning circulation. Nat. Geosci. 5, 813–816.

Liu, Z., Otto-Bliesner, B.L., He, F., Brady, E.C., Tomas, R., Clark, P.U., Carlson, A.E., Lynch-Stieglitz, J., Curry, W., Brook, E., Erickson, D., Jacob, R., Kutzbach, J., Cheng, J., 2009. Transient simulation of last deglaciation with a new mechanism for Bolling–Allerod warming. Science 325, 310–314.

Lyle, M., Wilson, P.A., Janecek, T.R., 2002. Leg 199 Summary. In: Proceedings of the Ocean Drilling Program Initial Reports, pp. 1–87.

Lynch-Stieglitz, J., Curry, W.B., Oppo, D.W., Ninneman, U.S., Charles, C.D., Munson, J., 2006. Meridional overturning circulation in the South Atlantic at the last glacial maximum. Geochem. Geophys. Geosyst. 7, Q10N03. http://dx.doi.org/10.1029/2005GC001226.

Marcott, S.A., Shakun, J.D., Clark, P.U., Mix, A.C., 2013. A reconstruction of regional and global temperature for the past 11,300 years. Science 339, 1198–1201.

Marshall, J., Donohoe, A., Ferreira, D., McGee, D., 2013. The ocean's role in setting the mean position of the atmosphere's ITCZ. Clim. Dyn. http://dx.doi.org/10.1007/s00382-013-1767-z.

McGee, D., deMenocal, P.B., Winckler, G., Stuut, J.B.W., Bradtmiller, L.I., 2013. The magnitude, timing and abruptness of changes in North African dust deposition over the last 20,000 yr. Earth Planet. Sci. Lett. 371–372, 163–176.

McManus, J.F., Francois, R., Gherardi, J.-M., Keigwin, L.D., Brown-Leger, S., 2004. Collapse and rapid resumption of Atlantic meridional circulation linked to deglacial climate changes. Nature 428, 834–837.

Meehl, G.A., Covey, C., Delworth, T., Latif, M., McAvaney, B., Mitchell, J.F.B., Stouffer, R.J., Taylor, K.E., 2007. The WCRP CMIP3 multimodel dataset – A new era in climate change research. Bull. Am. Meteorol. Soc. 88, 1383–1394.

Monnin, E., Indermuhle, A., Dallenbach, A., Fluckiger, J., Stauffer, B., Stocker, T.F., Raynaud, D., Barnola, J.M., 2001. Atmospheric CO_2 concentrations over the last glacial termination. Science 291, 112–114.

Muller, J., Kylander, M., Wust, R.A.J., Weiss, D., Martinez-Cortizas, A., LeGrande, A.N., Jennerjahn, T., Behling, H., Anderson, W.T., Jacobson, G., 2008. Possible evidence for wet Heinrich phases in tropical NE Australia: the Lynch's Crater deposit. Quat. Sci. Rev. 27, 468–475.

Partin, J.W., Cobb, K.M., Adkins, J.F., Clark, B., Fernandez, D.P., 2007. Millennial-scale trends in West Pacific warm pool hydrology since the Last Glacial Maximum. Nature 449, 452–455.

Peterson, L.C., Haug, G.H., Hughen, K.A., Rohl, U., 2000. Rapid changes in the hydrologic cycle of the tropical Atlantic during the last glacial. Science 290, 1947–1951.

Placzek, C., Quade, J., Patchett, P.J., 2006. Geochronology and stratigraphy of late Pleistocene lake cycles on the southern Bolivian Altiplano: Implications for causes of tropical climate change. Geol. Soc. Am. Bull. 118, 515–532.

Rashid, H., England, E., Thompson, L., Polyak, L., 2011. Late glacial to holocene Indian summer monsoon variability based upon sediment records taken from the Bay of Bengal. Terr. Atmos. Ocean. Sci. 22, 215.

Ritz, S.P., Stocker, T.F., Grimalt, J.O., Menviel, L., Timmermann, A., 2013. Estimated strength of the Atlantic overturning circulation during the last deglaciation. Nat. Geosci. 6, 208–212.

Robinson, L.F., Adkins, J.F., Keigwin, L.D., Southon, J., Fernandez, D.P., Wang, S.-L., Scheirer, D.S., 2005. Radiocarbon variability in the western North Atlantic during the last deglaciation. Science 310, 1469–1473.

Sachs, J.P., Sachse, D., Smittenberg, R.H., Zhang, Z., Battisti, D.S., Golubic, S., 2009. Southward movement of the Pacific intertropical convergence zone AD 1400–1850. Nat. Geosci. 2, 519–525.

Seltzer, G., Rodbell, D., Burns, S., 2000. Isotopic evidence for late quaternary climatic change in tropical South America. Geology 28, 35–38.

Shakun, J.D., Clark, P.U., He, F., Marcott, S.A., Mix, A.C., Liu, Z., Otto-Bliesner, B., Schmittner, A., Bard, E., 2012. Global warming preceded by increasing carbon dioxide concentrations during the last deglaciation. Nature 484, 49–54.

Stager, J.C., Ryves, D.B., Chase, B.M., Pausata, F.S.R., 2011. Catastrophic drought in the Afro-Asian monsoon region during Heinrich event 1. Science 331, 1299–1302.

Thornalley, D.J.R., Elderfield, H., McCave, I.N., 2010. Intermediate and deep water paleoceanography of the northern North Atlantic over the past 21,000 years. Paleoceanography 25, PA1211. http://dx.doi.org/10.1029/2009PA001833.

Trenberth, K.E., Caron, J.M., 2001. Estimates of meridional atmosphere and ocean heat transports. J. Climate 14, 3433–3443.

Vellinga, M., Wood, R.A., 2002. Global climatic impacts of a collapse of the Atlantic thermohaline circulation. Clim. Change 54, 251–267.

Vellinga, M., Wu, P., 2008. Relations between Northward Ocean and atmosphere energy transports in a coupled climate model. J. Climate 21, 561–575.

Voigt, A., Stevens, B., Bader, J., Mauritsen, T., 2013. The observed hemispheric symmetry in reflected shortwave irradiance. J. Climate 26, 468–477.

Waelbroeck, C., Paul, A., Kucera, M., Rosell-Melee, A., Weinelt, M., Schneider, R., Mix, A.C., Abelmann, A., Armand, L., Bard, E., Barker, S., Barrows, T.T., Benway, H., Cacho, I., Chen, M.T., Cortijo, E., Crosta, X., de Vernal, A., Dokken, T., Duprat, J., Elderfield, H., Eynaud, F., Gersonde, R., Hayes, A., Henry, M., Hillaire-Marcel, C., Huang, C.C., Jansen, E., Juggins, S., Kallel, N., Kiefer, T., Kienast, M., Labeyrie, L., Leclaire, H., Londeix, L., Mangin, S., Matthiessen, J., Marret, F., Meland, M., Morey, A.E., Mulitza, S., Pflaumann, U., Pisias, N.G., Radi, T., Rochon, A., Rohling, E.J., Sbaffi, L., Schafer-Neth, C., Solignac, S., Spero, H., Tachikawa, K., Turon, J.L., Members, M.P., 2009. Constraints on the magnitude and patterns of ocean cooling at the Last Glacial Maximum. Nat. Geosci. 2, 127–132.

Wang, X., Auler, A.S., Edwards, R.L., Cheng, H., Ito, E., Wang, Y., Kong, X., Solheid, M., 2007. Millennial-scale precipitation changes in southern Brazil over the past 90,000 years. Geophys. Res. Lett. 34. http://dx.doi.org/10.1029/2007GL031149.

Wang, X.F., Auler, A.S., Edwards, R.L., Cheng, H., Cristalli, P.S., Smart, P.L., Richards, D.A., Shen, C.C., 2004. Wet periods in northeastern Brazil over the past 210 kyr linked to distant climate anomalies. Nature 432, 740–743.

Wang, Y.J., Cheng, H., Edwards, R.L., An, Z.S., Wu, J.Y., Shen, C.C., Dorale, J.A., 2001. A high-resolution absolute-dated Late Pleistocene monsoon record from Hulu Cave, China. Science 294, 2345–2348.

Weldeab, S., Lea, D.W., Schneider, R.R., Andersen, N., 2007. 155,000 years of West African monsoon and ocean thermal evolution. Science 316, 1303–1307.

Xie, P.P., Arkin, P.A., 1996. Analyses of global monthly precipitation using gauge observations, satellite estimates, and numerical model predictions. J. Climate 9, 840–858.

Zhang, R., Delworth, T.L., 2005. Simulated tropical response to a substantial weakening of the Atlantic thermohaline circulation. J. Climate 18, 1853–1860.